EUROPEAN ORGANISATION FOR NUCLEAR RESEARCH

CERN/PPE 90-166
8 November 1990

PRODUCTION OF D_s^{*-} MESONS IN ANTINEUTRINO-NEON CHARGED CURRENT INTERACTIONS

A.E. Asratyan[7], P. Marage[3], M. Neveu[10], V.V. Ammosov[6], A.D. Andryakov[7], J.P. Baton[10], M. Berggren[11], V.S. Burtovoy[6], T. Coghen[5], O. Erriquez[1], G.S. Gapienko[6], J. Guy[9], G.T. Jones[2], V.S. Kaftanov[7], V.I. Klyukhin[6], V.A. Korotkov[6], S.P. Krutchinin[7], M.A. Kubantsev[7], I.V. Makhlueva[7], D.R.O. Morrison[4], P.V. Pitukhin[6], J. Sacton[3], K.E. Varvell[2], W. Venus[9], G. Wallenborn[3], S. Willocq[3*], W. Wittek[8] and V.G. Zaetz[6]

Abstract

Evidence of the production of the D_s^{*-} (2111) meson in $\overline{\nu}_\mu$Ne collisions is presented. The D_s^{*-} production rate times the $D_s^- \rightarrow \Phi\pi^-$ branching fraction is estimated to be $(2.3 \pm 0.7) \times 10^{-3}$ of all charged current events having a hadronic mass W above 3 GeV.

1 Dipartimento di Fisica dell'Universita e Sezione INFN, I–70126 Bari, Italy.
2 University of Birmingham, Birmingham B15 2TT, UK.
3 Inter-University Institute for High Energies, ULB–VUB, B–1050 Brussels, Belgium.
4 CERN, CH–1211 Geneva 23, Switzerland.
5 Institute of Nuclear Physics, PL–30055 Cracow, Poland.
6 Institute of High Energy Physics, Serpukhov, USSR.
7 Institute of Theoretical and Experimental Physics, Moscow, USSR.
8 Max-Planck-Institut für Physik und Astrophysik, D–8000 München 40, Germany.
9 Rutherford Appleton Laboratory, Chilton, Didcot, OX11 0QX, UK.
10 DPhPE, Centre d'Etudes Nucléaires, Saclay, F–91191 Gif sur Yvette, France.
11 Institute of Physics, University of Stockholm, S–11346 Stockholm, Sweden.

* Now at Tufts University, Medford, USA.

Submitted to Physics Letters B

1. Introduction

The charmed strange vector meson $D_s^{*\pm}$ (2111) has been studied extensively in e^+e^- experiments through its radiative decay $D_s^{*\pm} \rightarrow D_s^{\pm}\ \gamma$ to the lowest pseudoscalar state $D_s^{\pm}$ (1969) (see [1] and references therein). The subject of this paper is D_s^{*-} production in $\overline{\nu}_\mu$Ne charged current (CC) interactions.

The sample consists of some 23 000 CC events with a mean visible energy of 35 GeV and a muon of momentum over 4 GeV, selected with an external muon identifier. It is formed by combining the data collected with the 15–Foot Bubble Chamber at FNAL [2] with data from BEBC at CERN [3]. Combining the data is straightforward since the experimental conditions are very similar. Both experiments used bubble chambers filled with heavy neon-hydrogen mixtures and exposed to wide band antineutrino beams produced by 400 GeV protons. In both experiments, all charged current events were fully measured. After discarding bremsstrahlung photons and protons of momentum below 320 MeV, detailed comparison revealed very good compatibility between the two data sets.

2. Search for the signal : Method

To isolate the $D_s^{*-} \rightarrow D_s^-\gamma$ signal, we first select possible D_s^- mesons among various mass combinations, then search for a peak near 147.7 $\pm$ 1.7 MeV [1] in the gamma energy distribution in the D_s^- rest frame *. The D_s^- candidates are selected in the following channels:

$$D_s^- \rightarrow \Phi\pi^- \rightarrow K^+K^-\pi^- \tag{1}$$

$$D_s^- \rightarrow \Phi\pi^-\pi^0 \rightarrow K^+K^-\pi^-\gamma\gamma \tag{2}$$

$$D_s^- \rightarrow K^-K^{*0} \rightarrow K^-K^+\pi^- \tag{3}$$

$$D_s^- \rightarrow K^-K_s^0 \tag{4}$$

$$D_s^- \rightarrow K_s^0K_s^0\pi^- \tag{5}$$

The kaon mass hypothesis is considered for any charged particles of momentum greater than 200 MeV/c that have not been identified as pions or protons. The $\Phi(1020)$, $K^{*0}(890)$ and π^0 candidates were selected, respectively, as K^+K^- pairs with mass in the interval 1010–1030 MeV, $K^+\pi^-$ combinations in the interval 830–950 MeV and $\gamma\gamma$ pairs between

* Within the semi-inclusive approach taken in our preliminary studies [4], no complete D_s^- mass reconstruction was required. Additional studies revealed some inconsistencies in the semi-inclusive method, due to sensitivity to the choice of energy correction method.

115 and 155 MeV. Particles with relative momentum error $\Delta p/p$ above 30% were not considered. The mass resolution calculated from the data is about 5 MeV in the Φ region and the standard deviation of the observed π^0 peak is about 15 MeV. The mass of the D_s^- candidate is required to lie within two standard deviations of the D_s^- (1969) mass; ie we require $|\Delta m| < 2\sigma$, where σ is calculated for each event and is typically around 50 MeV but varies widely from event to event.

To reduce the combinatorial background, the following cuts are made.

i) The total event multiplicity (charged and neutral) is required to be under 15.

ii) For the channels (1–3) with two charged kaons, the selection $\cos\theta_{KK} > -0.75$ is applied, where θ_{KK} is the angle between the K^+K^- direction in the D_s^- candidate rest frame and the direction of the Lorentz boost from the lab system to the D_s^- rest frame. For channel (4), we demand $\cos\theta_K > -0.75$, where θ_K is a similarly defined K^- angle in the $K^-K_s^0$ rest frame. The motivation is that while the angular distribution is isotropic for the D_s^- decays, the pions wrongly called kaons are pushed towards the backward direction by the wrongly applied Lorentz boost. This cut approximately halves the combinatorial background while retaining 7/8ths of the signal.

iii) In channel (3), the D_s^- meson decay distribution being isotropic and the K^{*0} meson being a P-wave, the decay angular distribution has the form

$$dW \;/\; d\cos\theta \;\sim\; \cos^2\theta \tag{6}$$

where θ is the angle between the K^+ and K^- directions in the K^{*0} (or $K^+\pi^-$) rest frame. To suppress the combinatorial background in this channel further, we require $|\cos\theta| > 0.8$. According to (6), this should reject 51% of the K^{*0}'s from genuine D_s^- decays.

Having selected the D_s^- candidates, we consider the distribution of the energy E_γ^* of the gammas in the D_s^- rest frame. Only the "odd" gammas are used, *i.e.* those that do not form a π^0 mass combination in the range 115 to 155 MeV with any other gamma in the event. To ensure good detection efficiencies, only those odd gammas having momentum above 200 MeV/c are used. Gammas consistent with arising from muon inner bremsstrahlung are not included.

3. Search for the signal : Results

Fig. 1a shows the E_γ^* plot for the odd gammas under the condition $z > 0.75$, where z is the fraction of the visible hadron energy taken by the $D_s^-\gamma$ system (see below). An

enhancement is seen around $E^*_\gamma = 150$ MeV. Both its position and width agree well with those expected for the radiative $D_s^{*-} \to D_s^- \gamma$ signal, our rms resolution being 26 MeV in that region. The enhancement consists of 22 gammas, in the peak area $100 < E^*_\gamma < 200$ MeV, belonging to 21 events : these comprise six $\Phi\pi^-$ candidates, seven $\Phi\pi^-\pi^0$, seven $K^{*0}\ K^-$, no $K^-K^0_s$ and one $K^0_sK^0_s\pi^-$.

To estimate the background, we plot analogous E^*_γ distributions obtained by selecting mass combinations lying in the 'mass wings' located just outside the 'central regions' used above to select the good D_s^- , Φ and K^{*0} candidates. Figs. 1b–d show the results of selecting combinations in which

i) the mass of the D_s^- candidate lies in the mass wings, $2\sigma < |\Delta m| < 4\sigma$, instead of in the central region $|\Delta m| < 2\sigma$, but the mass of the Φ or K^{*0} candidate lies in the central region (Fig. 1b);

ii) either, for channels (1–2), the mass of the Φ candidate lies in the mass wings, *i.e.* m_{KK} lies in the interval (1000–1010) or (1030–1040) MeV, or, for channel (3), the mass of the K^{*0} candidate lies in the mass wings, *i.e.* $m_{K\pi}$ lies in the interval (770–830) or (950–1010) MeV, but in either case the mass of the D_s^- candidate lies in the central region (Fig. 1c);

iii) the mass of both the D_s^- candidate and the ϕ or K^{*0} candidate lies in the mass wings (Fig. 1d).

No peak around 150 MeV is observed in any of the background plots in Figs. 1b–d. Background (i), plotted in Fig. 1b, applies to all 5 channels; backgrounds (ii) and (iii), plotted in Figs. 1c and 1d, apply only to channels (1-3) containing pairs of kaons. The background is thus estimated to be 4.7 ± 1.5 events in the interval $100 < E^*_\gamma < 200$ MeV by taking the average of Figs. 1b, 1c and 1d for channels (1–3) and taking Fig. 1b alone for channels (4–5). Fig. 1a shows 21 events in this E^*_γ interval. Thus the signal amounts to (16.3 ± 4.7) events.

Using the same procedure, the estimated background amounts to 4.7 ± 1.7 events with E^*_γ below 100 MeV and 13.0 ± 2.3 with E^*_γ above 200 MeV, in good agreement with the numbers seen in Fig. 1a, namely 3 and 16 respectively. As a further check, the plots analogous to those of Figs. 1a–d, but with paired gammas instead of odd ones, are shown in Figs. 1e–h. Little or no signal is to be expected in these plots. Applying the same procedure to them yields an excess of 0.7 ± 2.2 events, consistent with zero, in the region $100 < E^*_\gamma < 200$ MeV of Fig. 1e.

We therefore conclude that most of the events in the peak region in Fig. 1a arise from

$D_s^{*-} \to D_s^- \gamma$ decays. To check the consistency of this interpretation, we look in other ways for the Φ and D_s^- signals they should contain:

i) Fig. 2a shows the K^+K^- mass distributions obtained by relaxing the Φ mass cut, for D_s^- candidates in the central region. Fig. 2b shows the corresponding background plots, using the D_s^- mass wings. Their comparison confirms the presence of a clear Φ signal.

ii) Similarly, Fig. 3a shows the $\Phi\pi^-$, $\Phi\pi^-\pi^0$ and $K^{*0}\ K^-$ mass distributions expressed in terms of standard deviations from the D_s^- (1969) mass, obtained by relaxing the D_s^- mass constraint. Fig. 3b shows the corresponding background plot using the Φ or K^{*0} mass wings. A clear D_s^- signal is seen in Fig. 3a.

Furthermore, the Φ and D_s^- signals in Figs. 2a and 3a contain the numbers of events expected from the analysis of Fig. 1a.

The contamination of the signal by the production of the charmed non-strange $D^{*-}(2010)$ meson and its subsequent cascade decay $D^{*-} \to D^-\gamma$, $D^- \to K^{*0}\pi^-$ and $K^{*0} \to K^+\pi^-$ is estimated to be less than one event, even if the $D^-(1869)$ is fully reflected into a D_s^- (1969) when the π^- is taken as a K^-, since the product of the three branching fractions is only $\sim 3 \times 10^{-3}$ [5].

4. D_s^{*-} production characteristics

The kinematical characteristics of the events in the E_γ^* peak are shown in Table 1. For comparison, Table 1 also gives the characteristics of the events contributing to a wider interval $0 < E_\gamma^* < 300$ MeV of the plots in Fig. 1, with the peak events excluded. The signal events appear to be less energetic than the background events. No other differences are found at the available statistical level.

The analysis made above for $z > 0.75$ has been repeated for two other z intervals. The results are shown in Figs. 4a and 4b for odd and paired gammas. The signal is seen to be concentrated at z values larger than 0.75 in Fig. 4a, for odd gammas.

Deep-inelastic D meson production by neutrinos [6] typically has a pronounced increase in rate with neutrino energy and a rather wide z distribution ($< z > \approx 0.6$). Qualitatively, for D_s^{*-} production we observe a harder z distribution and a softer E_ν distribution than for D production. This suggests a difference in the production mechanism.

In the framework of the Vector Meson Dominance model [7,8] a virtual D_s^{*-} meson has a direct Cabbibo–favoured coupling to the W–boson and then scatters, elastically or

inelastically, on a nucleon. Some of the signal should then be diffractive. A search for the $D_s^{*-} \rightarrow D_s^- \gamma$ signal was made with no explicit z selection amongst events containing no negative particles apart from those from the D_s^- decay. It gave results very similar to those described above. To search for a diffractive contribution, the $D_s^{*-} \rightarrow D_s^- \gamma$ events without additional negative particles satisfying the condition $|t| - t_{\rm min} < 0.6$ GeV^2 were selected. Four possible diffractive candidates were found. Their characteristics are given in Table 2. The background is less than one event. This might indicate the presence of a diffractive contribution at the level of some 25% of the total signal.

The single $K^{*-} K_s^0$ event listed in Table 2 is perhaps of particular interest. It is a $\mu^+ \; p \; K_1^0 \; K_2^0 \; \pi^- \; \gamma$ final state (with particle momenta 4429, 387, 6708, 8378, 489 and 1475 MeV/c respectively), compatible with the reaction

$$\overline{\nu}_\mu \; p \; \rightarrow \; \mu^+ \; D_s^{*-} \; p \tag{7}$$

with $m(K_1^0 K_2^0 \pi^-) = 1990 \pm 29$ MeV, $m(K_2^0 \pi^-) = 883 \pm 17$ MeV, $|\cos \theta| = 0.65$ (a fairly typical angle for $K^{*0} \; K^-$, see (6)), and $E_\gamma^* = 140$ MeV. In this event, the strange particles are uniquely identified.

5. D_s^{*-} production rate

To estimate the D_s^{*-} production rate, we use the existing data on the D_s^- branching fractions relative to the $D_s^- \rightarrow \Phi \pi^-$ branching fraction [9–13]:

$$B(\Phi \pi^- \pi^0) \; / \; B(\Phi \pi^-) \; = \; 2.4 \; \pm \; 1.1 \qquad [9] \tag{8}$$

$$B(K^{*0} K^-) \; / \; B(\Phi \pi^-) \; = \; 0.96 \; \pm \; 0.11 \qquad [10-13] \text{ averaged} \tag{9}$$

$$B(K^- K^0 \;) \; / \; B(\Phi \pi^-) \; = \; 0.98 \; \pm \; 0.18 \qquad [12,13] \text{ averaged} \tag{10}$$

$$B(K^{*-} K^0) \; / \; B(\Phi \pi^-) \; = \; 1.20 \; \pm \; 0.22 \qquad [13] \tag{11}$$

Using these values we can estimate the product of the D_s^{*-} production rate per charged current event, R, and the $D_s^- \rightarrow \Phi \; \pi^-$ branching fraction. Taking account of the π^0 and K_s^0 detection efficiencies (taken as 0.30 and 0.50 respectively), the loss of badly measured tracks (correction factor 1.1 per charged hadron track), the relevant Φ and K^* branching fractions and the acceptances of the cuts listed above, the overall detection efficiencies for the five D_s^- decay channels are estimated to be 0.33 for $\Phi \pi^-$, 0.10 for $\Phi \pi^- \pi^0$, 0.22 for $K^{*0} \; K^-$, 0.20 for $K^0 K^-$ and 0.04 for $K^{*-} K^0$. After applying these correction factors, the ratios of events in other channels to events in the $\Phi \pi$ channel agree reasonably well with

the ratios of branching ratios given above. Taking into account also the gamma detection efficiency (taken as 0.60) and the event scanning efficiencies, the D_s^{*-} production rate per charged current event times the $D_s^- \rightarrow \Phi\,\pi^-$ branching fraction is

$$R\,(z\,>\,0.75)\,\cdot\,B(\phi\,\pi^-)\,=\,(1.08\,\pm\,0.34)\times 10^{-3} \tag{12}$$

or

$$R\,(z>0.75,\;W>3\;\mathrm{GeV})\,\cdot\,B(\phi\,\pi^-)\,=\,(2.3\,\pm\,0.7)\times 10^{-3} \tag{13}$$

per charged current event with corrected hadron system mass W above the threshold value of 3 GeV.

The absolute branching fraction of the $D_s^- \rightarrow \Phi\,\pi^-$ decay is poorly known. An estimate from e^+e^- experiments is ~3.5%, which could be wrong by a factor of two because of systematic uncertainties [14]. While the 90% c.l. upper limit on $B(\phi\,\pi^-)$ imposed by MARK III is as restrictive as 4.1% [15] and CLEO have reported a value of $(3.1 \pm 0.6^{+0.9}_{-0.6} \pm 0.6)\%$ [16], a 90% c.l. lower limit of 3.4% has been obtained by the E691 collaboration [17] and the analysis performed by the ACCMOR group suggests a higher value of $(6.0^{+2.1}_{-1.6})\%$ [18]. Using 4.5% as a representative value would give $R\,(z>0.75)\,=\,0.024\,\pm\,0.008$, or

$$R\,(z>0.75,\;W>3\;\mathrm{GeV})\,=\,(0.051\,\pm\,0.016) \tag{14}$$

which is an appreciable fraction of the overall charm production.

6. Conclusion

Production of the D_s^{*-} (2111) meson in antineutrino interactions has been observed through its radiative decay $D_s^{*-} \rightarrow D_s^-\gamma$ with D_s^- subsequently decaying mainly into $\Phi\pi^-$, $\Phi\pi^-\pi^0$ and $K^{*0}K^-$. The production rate times the $D_s^- \rightarrow \Phi\,\pi^-$ branching fraction is estimated to be $(2.3\,\pm\,0.7)\times 10^{-3}$ per charged current event with hadronic mass W above 3 GeV.

Acknowledgements

We are indebted to the accelerator and neutrino beam and bubble chamber staffs at Fermilab and CERN and to our other colleagues in the E180 and WA59 collaborations and to all our scanning and measuring personnel whose work helped to produce these data.

Table 1 : Comparison of mean values of visible quantities between peak events and background events. The peak events are the 21 events that contribute to the 22 entries in Fig. 1a with E^*_γ between 100 and 200 MeV. The background events are the other 57 events that contribute entries in any of Figs. 1(a-h) with E^*_γ below 300 MeV.

	Peak events	Background events
E_ν (GeV)	26.1 $\pm$ 3.0	38.2 $\pm$ 3.2
ν (GeV)	11.1 $\pm$ 1.7	14.2 $\pm$ 1.5
W (GeV)	3.96 $\pm$ 0.34	4.53 $\pm$ 0.23
Q^2 (GeV^2)	3.87 $\pm$ 0.79	4.41 $\pm$ 0.39
x_B	0.23 $\pm$ 0.04	0.21 $\pm$ 0.02
y_B	0.43 $\pm$ 0.04	0.40 $\pm$ 0.03
Charged multiplicity	6.5 $\pm$ 0.3	6.2 $\pm$ 0.2
Gamma multiplicity	2.8 $\pm$ 0.3	2.9 $\pm$ 0.2
D_s^- momentum (GeV/c)	8.5 $\pm$ 0.9	9.0 $\pm$ 0.7

Table 2 : Characteristics of the four diffractive candidates.

Mode	$\|t\|$	$t_{\min}$	E_ν	ν	Q^2
$K^{*-}K^0_s$	0.61	0.04	21.9	17.5	2.03
$\Phi\pi^-$	1.13	1.09	31.1	8.4	6.43
$\Phi\pi^-\pi^0$	0.33	0.30	14.5	6.5	0.95
$K^{*0}K^-$	0.73	0.56	22.1	6.0	0.73

References

[1] H. Albrecht et al., Phys. Lett. 207B, 349 (1988)

[2] P.A. Goritchev et al., Sov. J. Nucl. Phys. 39, 396 (1984)

[3] W. Wittek et al., Z. Phys. C40, 231 (1988)

[4] A.E. Asratyan et al., Phys. Lett. 156B, 441 (1985)
A.E. Asratyan et al., preprint IIHE 89–06 (1989)

[5] J. Adler et al., Phys. Lett. 208B, 152 (1988)
J. Adler et al., Phys. Rev. Lett. 62, 1821 (1989)

[6] N. Ushida et al., Phys. Lett. 206B, 380 (1988)

[7] B.A. Arbuzov et al., Sov. J. Nucl. Phys. 21, 682 (1975)

[8] M.-S. Chen et al., Nucl. Phys. B118, 345 (1977)

[9] J.C. Anjos et al., Phys. Lett. 223B, 267 (1989)

[10] H. Albrecht et al., Phys. Lett. 179B, 398 (1986)

[11] J.C. Anjos et al., Phys. Rev. Lett. 60, 897 (1988)

[12] J. Adler et al., Phys. Rev. Lett. 63, 1211 (1989)

[13] W.-Y. Chen et al., Phys. Lett. 226B, 192 (1989)

[14] R.J. Morrison, J. Rollin and M.S. Witherell, UCSB–HEP–89–01 (1989)

[15] J. Adler et al., Phys. Rev. Lett. 64, 169 (1990)

[16] J. Alexander et al., Phys. Rev. Lett. 65, 1531 (1990)

[17] J.C. Anjos et al., Phys. Rev. Lett. 64, 2885 (1990)

[18] S. Barlag et al., Z. Phys. C48, 29 (1990)

Figure Captions

Fig. 1 Distributions of the gamma energy E^*_γ in the D_s^- rest frame for:
(a) odd gammas, D_s^- central region, channels 1–5;
(b) odd gammas, D_s^- mass wings, channels 1–5;
(c) odd gammas, D_s^- central region, Φ/K^{*0} mass wings, channels 1–3;
(d) odd gammas, D_s^- mass wings, Φ/K^{*0} mass wings, channels 1–3.
Distributions (e–h) are the same as (a–d) but for paired gammas instead of odd ones.
The numbers in the histograms indicate the channel, as defined in the text.

Fig. 2 Distributions of $m(K^+K^-)$ for the $K^+K^-\pi^-$ and $K^+K^-\pi^-\pi^0$ combinations with $\cos\theta_{KK} > -0.75$ tagged by an odd gamma with $100 < E^*_\gamma < 200$ MeV:
(a) D_s^- central mass region, (b) D_s^- mass wings.

Fig. 3 Mass distributions in units of standard deviations from the D_s^- (1969) mass for the $\Phi\pi^-$, $\Phi\pi^-\pi^0$ and $K^{*0}K^-$ combinations tagged by an odd gamma with $100 < E^*_\gamma < 200$ MeV: (a) Φ/K^{*0} central mass region, (b) Φ/K^{*0} mass wings.

Fig. 4 Fractional hadron energy distribution of the observed enhancement (see text) for:
(a) odd gammas, (b) paired gammas.

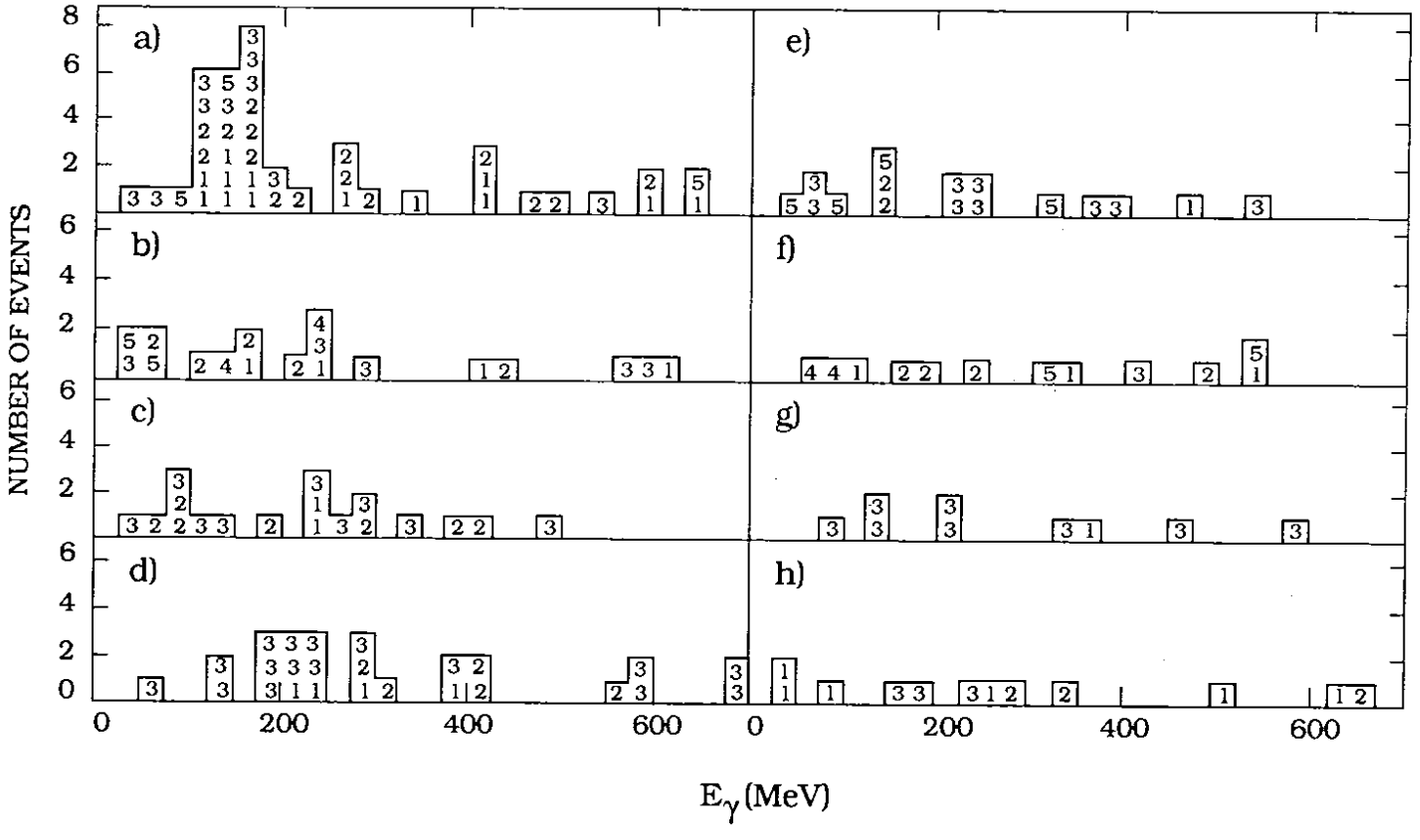

Fig. 1

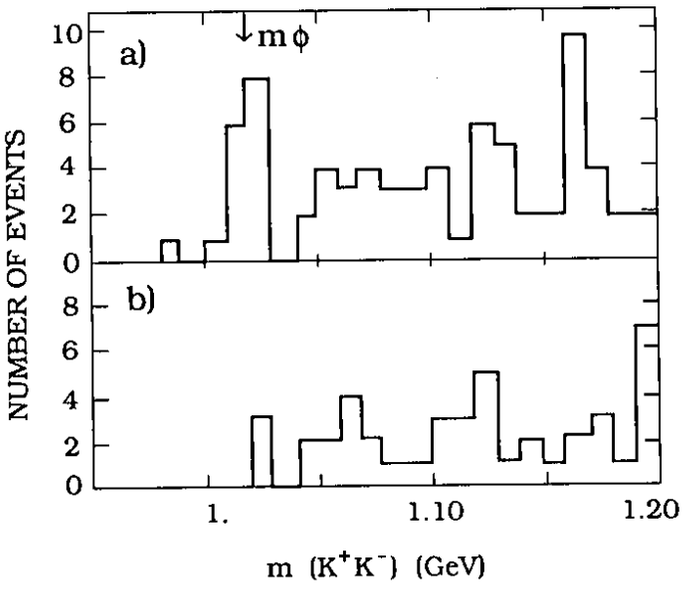

Fig.2

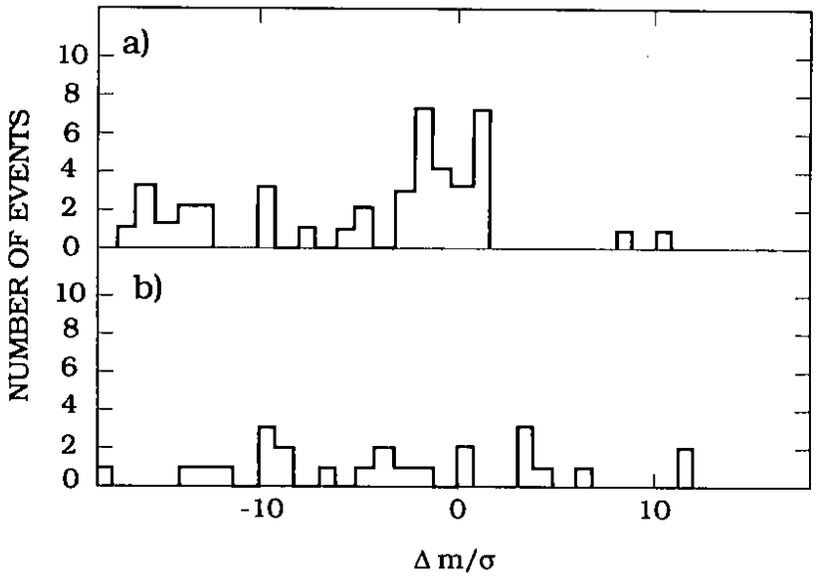

Fig.3

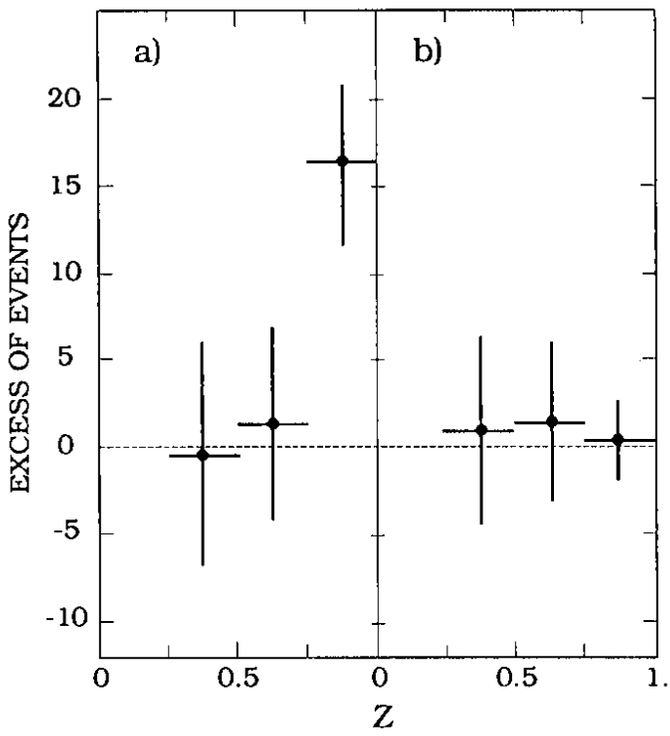

Fig.4

Imprimé au CERN. Prix : 0.40 Fr.